ChemComm

FEATURE ARTICLE

View Article Online
View Journal | View Issue

Cite this: *Chem. Commun.*, 2022, **58**, 171

Advances in allylic and benzylic C–H bond functionalization enabled by metallaphotoredox catalysis

Huifeng Yue, †*[a] Chen Zhu, †*[a] Long Huang,[b] Abhishek Dewanji[b] and Magnus Rueping *[a]

Received 7th November 2021,
Accepted 6th December 2021

DOI: 10.1039/d1cc06285a

rsc.li/chemcomm

Metallaphoto-catalysis has been established as a robust platform for efficient construction of a range of chemical bonds. Moreover, transformation of native functionalities such as C(sp^3)–H bonds to produce functional molecules represents one of the most attractive strategies in organic synthesis. Merging two powerful methodologies, metallaphoto-catalyzed benzylic and allylic C(sp^3)–H bond functionalizations provide a series of general and mild approaches for diversification of alkylbenzenes and alkenes.

1. Introduction

Transformation of native functionalities to produce high value-added compounds has always been a critical goal pursued by chemists studying organic catalysis and synthesis. C–H bonds are among the most ubiquitous chemical bonds in nature; therefore, direct functionalization of such bonds is of great significance due to its step and atom economy. The last few decades have witnessed the development of methodologies for C(sp^2)–H bond activation, and a wide range of valuable organic compounds have been accessed *via* these powerful advancements.[1–9] Due to the abundance of starting materials such as hydrocarbons, greater emphasis has been placed on functionalization of C(sp^3)–H bonds in recent years, and both C–C and C-heteroatom bond formation has been achieved *via* different catalytic approaches.[10–17] Despite these advancements, a number of limitations remain, most notably associated with the use of precious metals with relatively high loadings or the need for directing groups, stoichiometric oxidants, or high temperatures.

Over the past decade, photocatalysis has proven to be a powerful platform for a wide range of organic transformations that would otherwise be unavailable.[18–25] In particular, photoredox-catalyzed C–H bond functionalization has been established, and it allows site-selective activation of inert alkanes.[26–28] Further combination of photocatalysis with transition metals in C–H bond activation enabled a wide range of cross-coupling reactions using hydrocarbons as coupling partners.[29–31] Given that the number of publications on metallaphoto-catalyzed allylic and benzylic C–H bond functionalization is rapidly increasing, this feature article will mainly focus on newly developed protocols in this area. In general, alkyl radicals can be delivered *via* hydrogen atom transfer (HAT) between the alkyl benzene/alkene and the excited photocatalyst, or HAT reagents. Direct oxidation of alkenes by excited photocatalysts and subsequent deprotonation could also afford allylic radicals. The resulting allylic or benzylic radical could then react with a variety of metal catalysts. These newly established protocols are categorized based on the types of products they generate: (1) arylation and alkenylation of benzylic and allylic C(sp^3)–H bonds; (2) acylation of benzylic and allylic C(sp^3)–H bonds; (3) alkylation of benzylic and allylic C(sp^3)–H bonds; (4) carboxylation of benzylic and allylic C(sp^3)–H bonds; (5) alkynylation of benzylic and allylic C(sp^3)–H bonds; and (6) sulfonylation and azidation of benzylic and allylic C(sp^3)–H bonds. We believe that this classification will help the community understand this type of reaction systematically and will be beneficial to further development of more diverse benzylic and allylic C(sp^3)–H bond functionalization methodologies under mild conditions (Scheme 1).

2. Arylation and alkenylation of benzylic and allylic C(sp^3)–H bonds

The construction of C(sp^3)–C(sp^2) bonds has long been a vital aspect of increasing molecular complexity. In this context, elegant studies on photoredox and nickel dual-catalyzed arylation of unactivated C(sp^3)–H bonds were reported in 2016 by MacMillan, Doyle, and Molander, who realized C(sp^3)–H activation of amines and ethers, respectively.[32–34] For each protocol,

[a] *KAUST Catalysis Center, KCC, King Abdullah University of Science and Technology, KAUST, Thuwal 23955-6900, Saudi Arabia. E-mail: magnus.rueping@kaust.edu.sa*
[b] *Institute of Organic Chemistry, RWTH Aachen University, Landoltweg 1, 52074 Aachen, Germany*
† These authors contributed equally to this work.

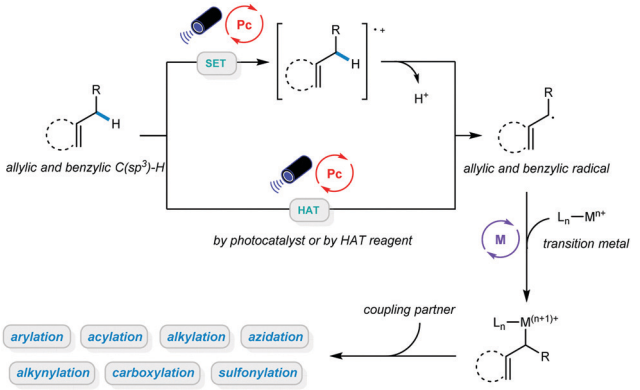

Scheme 1 Metallaphoto-catalyzed allylic and benzylic C–H bond functionalization.

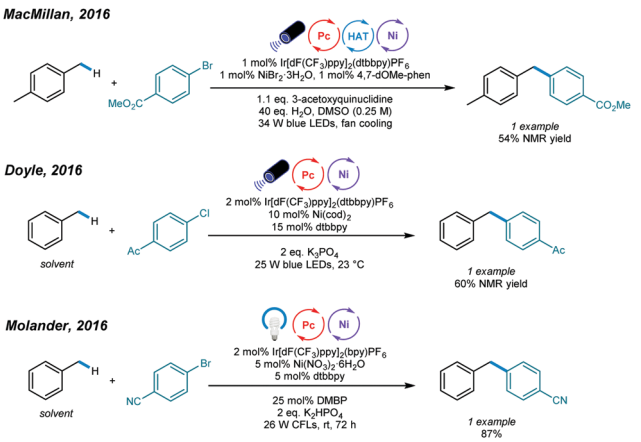

Scheme 2 Photoredox and nickel dual-catalyzed arylations of unactivated C(sp^3)–H bonds.

one example of benzylic C(sp^3)–H arylation of toluene was provided (Scheme 2).

One year later, an interesting UV light-induced benzylic C–H arylation of methylbenzenes *via* nickel catalysis was developed by Murakami and coworkers (Scheme 3).[35] In this catalytic system, 5.0 mol% of $NiCl_2$·dtbbpy complex and 365 nm UV light were used. The catalytic cycle starts with UV light-induced homolysis of $NiCl_2$·dtbbpy, which generates the active Ni^I–X catalyst. Oxidative addition of an aryl bromide gives an Ar–Ni^{III}(X)–Br intermediate that is transformed to [Ar–Ni^{III}(X)–Br]* upon irradiation with UV light. Homolysis of the resulting Ni^{III} species gives an Ar–Ni^{II}–Br intermediate and X$^\bullet$ radical. The X$^\bullet$ radical quickly abstracts one H atom to produce the benzyl radical that is trapped by Ar–Ni^{II}–Br to form a reactive Bn–Ni^{III}(Br)–Ar intermediate. Reductive elimination from the unstable Ni^{III} species delivers the product and regenerates the active Ni^I–X catalyst. UV-vis absorption spectra of the components rationalizes the proposed mechanism. The scope with regard to aryl bromides was broad, as illustrated by tolerance of electron-withdrawing and electron-donating groups, including trifluoromethyl, fluoro, chloro, ester, cyano, pyridine, thiophene, and even reactive boronic esters. A series of toluene

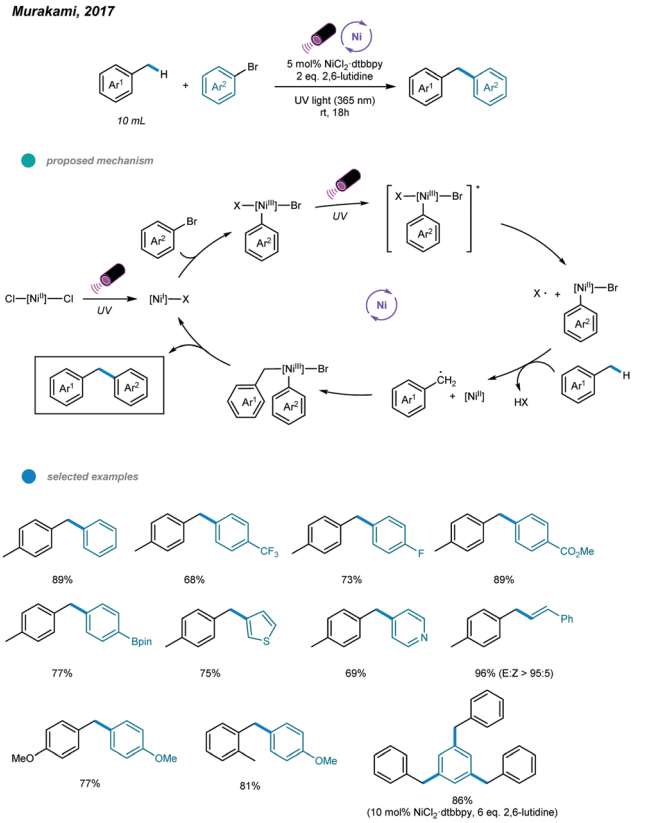

Scheme 3 UV light-induced nickel-catalyzed benzylic C–H arylations of methylbenzenes.

derivatives served as feasible coupling partners. Additionally, tribenzylbenzene was obtained from tribromobenzene in a single operation with a high yield.

Although arylation of benzylic C(sp^3)–H bonds has been realized, arylation of allylic C(sp^3)–H bonds remained undeveloped. To address this issue, Rueping and coworkers developed a photoredox and nickel dual-catalyzed protocol realizing cross-coupling of allylic C(sp^3)–H bonds with aryl and vinyl bromides in 2018 (Scheme 4).[36] A series of highly valuable allylarenes and 1,4-dienes were obtained from unactivated alkenes under mild conditions. The methodology features the first combination of an inexpensive acridinium photocatalyst and a nickel-metal catalyst. Mechanistically, irradiation with blue light excites the photocatalyst Mes–Acr–Me$^+$ to give excited [Mes–Acr–Me$^+$]*, which undergoes triplet–triplet energy transfer with Ar–Ni^{II}–Br to form an electronically excited [Ar–Ni^{II}–Br]* species. Then, the excited Ni^{II} species undergoes homolysis to give a bromine radical that abstracts a hydrogen atom from the allylic C(sp^3)–H bond of an olefin, generating an allylic radical. Addition of the allylic radical to the active Ni^I species affords a Ar–Ni^{II}–allylic intermediate, and reductive elimination delivers the coupled product. Radical trapping experiments with TEMPO and UV light control experiments were carried out and support this mechanism. A wide range of electron-deficient aryl bromides and heterocyclic substrates worked well in this allylation system, giving the corresponding products in moderate to excellent yields.

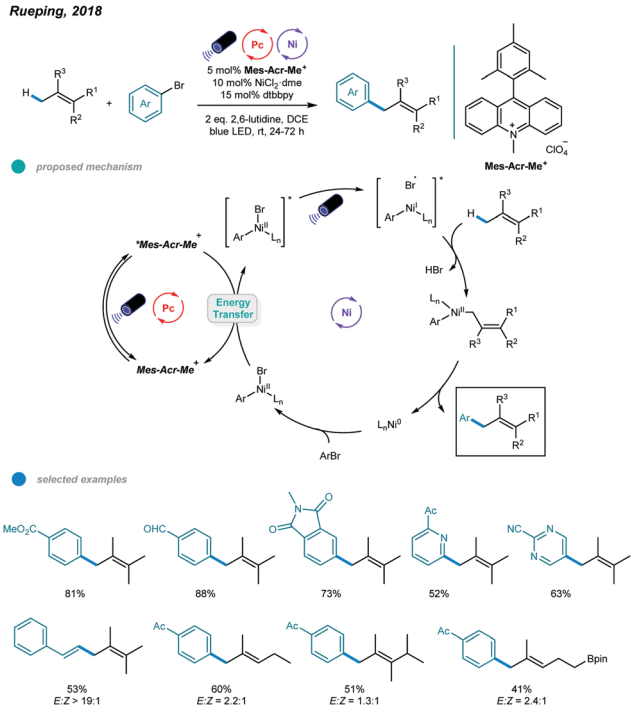

Scheme 4 Photoredox and nickel dual-catalyzed allylic C(sp^3)–H arylations and vinylations.

Additionally, vinyl bromides reacted smoothly with alkenes, providing an efficient way to construct valuable 1,4-dienes with good stereoselectivity. In addition, a series of tri- and tetrasubstituted alkenes participated and provided moderate to good yields. Notably, the reactions exhibit excellent regioselectivities, and coupling tends to replace primary C–H bonds rather than methylene and methine C–H bonds. Additionally, monoarylation adducts were observed exclusively, which may be due to steric effects. The problems remaining to be addressed are the use of electron-rich aryl bromides and achieving *Z*/*E* control when using asymmetric alkenes as coupling partners.

Making use of a diaryl ketone photosensitizer, Rueping and coworkers later extended the arylation scope to benzylic C(sp^3)–H bonds and established a photo/nickel dual catalyzed method for direct arylation of toluene derivatives (Scheme 5).[37] The use of benzophenone enables generation of benzylic radicals from toluene, and the resulting benzylic radicals then participate in the nickel catalytic cycle and form a series of diarylmethanes. As to the mechanism, photoexcitation of the diaryl ketone photosensitizer PS produces the excited triplet state PS*, which abstracts a H atom from toluene and gives a benzyl radical that subsequently adds to the active Ni^0 species to form a Bn–Ni^I intermediate. Oxidative addition of an aryl halide to the resulting Ni^I species leads to formation of an unstable Bn–Ni^{III}Br–Ar intermediate that tends to undergo reductive elimination to deliver the coupling product and Ni^I–Br. Reduction of this Ni^I-Br by reduced PS (PS–H) with the aid of a base regenerates the active Ni^0 catalyst and completes the catalytic cycle. An array of aryl bromides bearing electron-withdrawing and electron-donating groups reacted

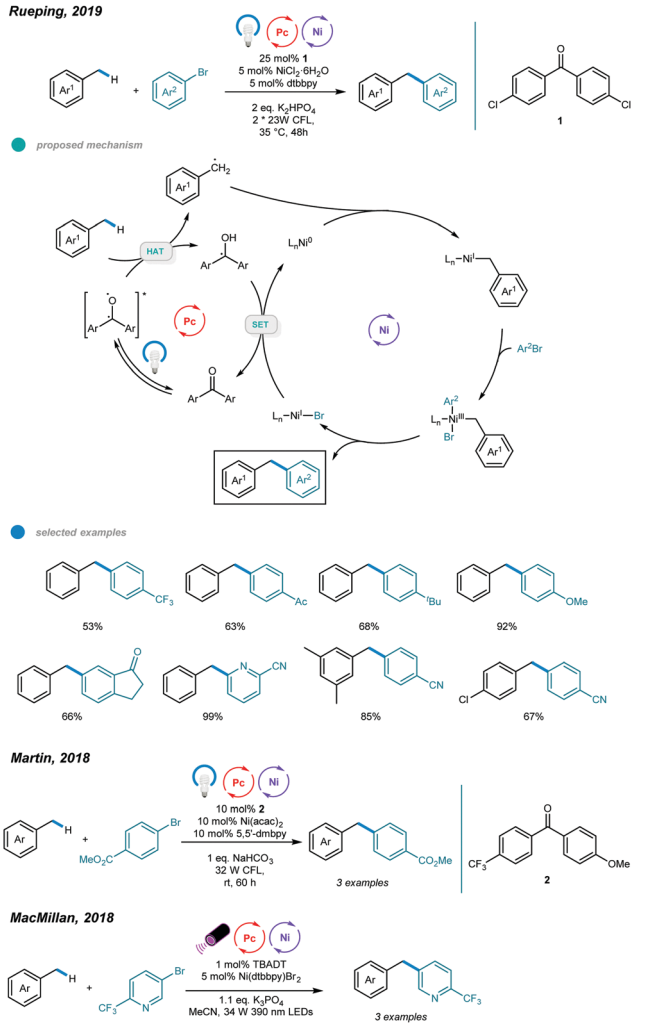

Scheme 5 Photoredox and nickel dual-catalyzed benzylic C(sp^3)–H arylations of toluene derivatives.

with toluene smoothly, affording the corresponding diarylmethanes in moderate to excellent yields.

Substrates with fused rings and heterocycles also underwent this transformation and showed good yields. The reaction occurred at the C–Br bond for 4-chlorobromobenzene, and the bromotolyl benzylic radical was not observed, indicating good chemoselectivity for this benzylic arylation. Notably, steric hindrance has little influence on reaction activity. In addition, electron-deficient and heterocyclic aryl chlorides were also suitable for this transformation. Xylenes and mesitylene also showed excellent reactivity. When applying the standard reaction conditions to aryl iodides, the reactivity was much lower. Interestingly, the addition of one equivalent of tetrabutyl ammonium bromide (TBAB) as an additive improved the yields significantly. These results, together with those of control experiments, indicate that the diaryl ketone photosensitizer acts as both a hydrogen atom transfer agent and an energy transfer agent. Moreover, scale-up was performed and proceeded with high yield. The use of alkylbenzenes other than methyl benzenes seems ineffective in this protocol. It is noted that the MacMillan and Martin

groups also independently reported nickellaphoto-catalyzed arylation of C(sp^3)–H bonds, and three examples of alkylbenzenes were presented (Scheme 5).[38,39]

Very recently, Lee and coworkers realized the benzylic C(sp^3)–H arylations of indole derivatives (Scheme 6).[40] The facile oxidation of indoles enabled the efficient generation of the benzylic radical *via* a sequential electron transfer–proton transfer (ET/PT). Particularly, the radical cation was first generated *via* the oxidation of the indole by the excited Ir-based photocatalyst, followed by the deprotonation to give the benzylic radical. The resulting benzylic radical was trapped by the active Ni^0 catalyst to deliver a Ni^I complex, which undergoes oxidative addition with aryl bromide to afford a Ni^{III} complex. Next, the unstable Ni^{III} complex undergoes facile reductive elimination to furnish the arylation product and Ni^I–Br species that is reduced to regenerate the active Ni^0 catalyst. The scope regarding to both indole substrates and aryl bromides are broad with even complex drug molecule derivatives applicable. However, other types of heterocycles including benzofuran, thiophene and pyrrole failed to give to desired products.

Although these protocols provide efficient ways to realize functionalization of allylic or benzylic C–H bonds, they are limited to achiral processes, which may be due to the lack of

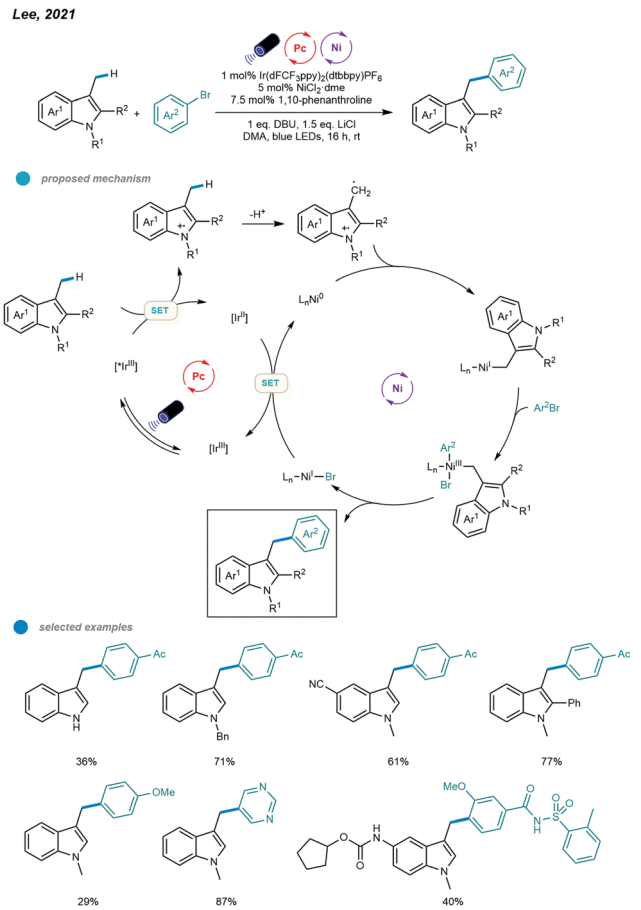

Scheme 6 Photoredox and nickel dual-catalyzed benzylic C(sp^3)–H arylation of indole derivatives.

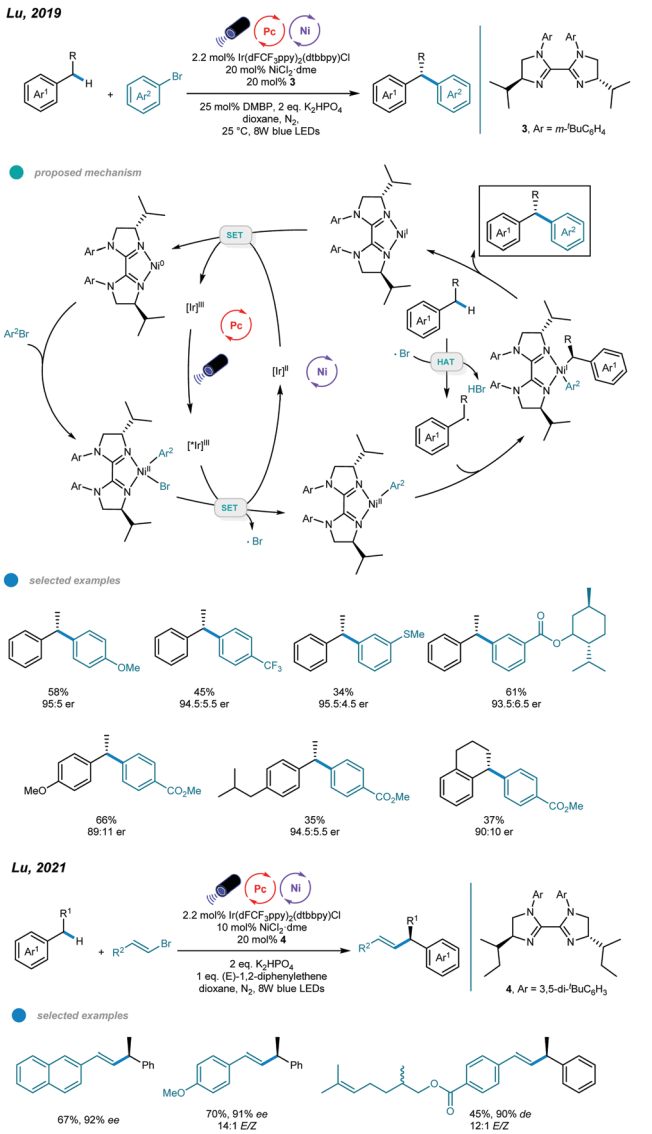

Scheme 7 Photoredox and nickel dual-catalyzed enantioselective benzylic C(sp^3)–H arylation of alkylbenzenes.

efficient chiral ligands. To address this issue, Lu and coworkers designed a series of chiral biimidazoline (BiIM) ligands and realized enantioselective benzylic C(sp^3)–H arylation of alkylbenzenes with aryl bromides (Scheme 7).[41] Similarly, oxidative addition of aryl halide to the Ni^0 species generated *in situ* provides an Ar–Ni^{II}–Br complex, which is oxidized by the excited $*Ir^{III}$ catalyst to give a new Ar–Ni^{II} species and Br• radical. The Br• radical abstracts a hydrogen atom from the alkylbenzene to generate a benzylic radical that subsequently adds to the Ar–Ni^{II} species to afford a Ni^{III} complex. Then, the chiral 1,1-diaryl alkane product is produced *via* reductive elimination from the Ni^{III} complex, which also yields a Ni^I intermediate. SET occurs between the Ni^I intermediate and the reducing Ir^{II} species, regenerating the Ni^0 species and the ground state Ir^{III} photocatalyst. After optimization, the authors found that addition of bis(4-methoxyphenyl)methanone (DMBP) as a cophotocatalyst improved the yield, and the use of sterically

hindered *N*-3-^{t}BuPh-^{i}PrBiIM gave the highest yield and ee value. Electron-rich and electron-deficient aryl bromides, as well as polycyclic and heterocyclic aryl bromides, all afforded the corresponding chiral 1,1-diaryl alkanes in moderate to good yields and with good enantioselectivity. A number of substituted benzenes (4 equivalents) underwent this asymmetric benzylic C–H arylation, and moderate yields with good ers were observed after 96 h. It should be noted that only secondary benzylic C–H bonds could be arylated, and tertiary benzylic C–H bonds were unreactive in this protocol. Later, the same group also developed the photoredox and nickel dual catalyzed stereo- and enantioselective benzylic C–H alkenylation (Scheme 7).[42] A wide range of chiral allylic compounds were obtained in up to 93% ee and $>20/1$ *E*/*Z* ratio. The high stereoselectivity attributes to the skillful use of stilbene as a triplet-energy inhibitor, which declines photocatalytic *E*/*Z* isomerization of the product.

3. Acylation of benzylic C(sp^3)–H bonds

Ketones and esters are two of the most important and useful classes of compounds in organic chemistry. Accordingly, efficient methods for preparation of these functional groups are always desirable. In 2018, the Doyle group developed a photoredox and nickel dual-catalyzed protocol for acylation of unactivated C–H bonds in alkanes and toluene derivatives (Scheme 8).[43]

Various carbonyl derivatives were obtained *via* site-selective cross-coupling of acyl chlorides and hydrocarbons. The reaction starts with oxidative addition of a chloroformate derivative to Ni^0, generating a $Ni^{II}(CO_2R)(Cl)$ complex that is then oxidized by the excited $^*Ir^{III}$ photocatalyst to form a Ni^{III} intermediate. The Cl$^\bullet$ radical is then generated *via* photoelimination from the Ni^{III} intermediate upon irradiation with blue light. Hydrogen atom abstraction of hydrocarbons by Cl$^\bullet$ radicals leads to a carbon-centered radical that was trapped by the Ni^{II} intermediate to afford an unstable Ni^{III} intermediate. The acylation product is produced *via* reductive elimination from the resulting Ni^{III} intermediate and a Ni^{I} intermediate is generated. Finally, the active Ni^0 catalyst is regenerated *via* reduction of the Ni^{I} intermediate by the reducing Ir^{II} photocatalyst. Notably, in addition to toluene, other acyclic and cyclic alkyl benzenes all gave the acylated product with good efficiency and regioselectivity. The utilization of air-sensitive $Ni(cod)_2$ necessitates further improvement.

Another methodology for the synthesis of unsymmetrical ketones was developed by Rueping and coworkers. They realized a photoinduced nickel-catalyzed benzylic C–H acylation reaction using 4-benzoylphenyl acetate as a photosensitizer (Scheme 9).[44] A series of unsymmetrical ketones were prepared *via* cross-coupling of methylbenzenes with acid chlorides and anhydrides. The mechanism is similar to that for benzylic C–H arylation. Both aromatic and aliphatic acid chlorides were successfully converted to the corresponding ketones with moderate to high efficiency. The steric hindrance of methylbenzene significantly affected the reactivity of the transformation, as illustrated by the fact that *ortho*-xylene furnished the acylation

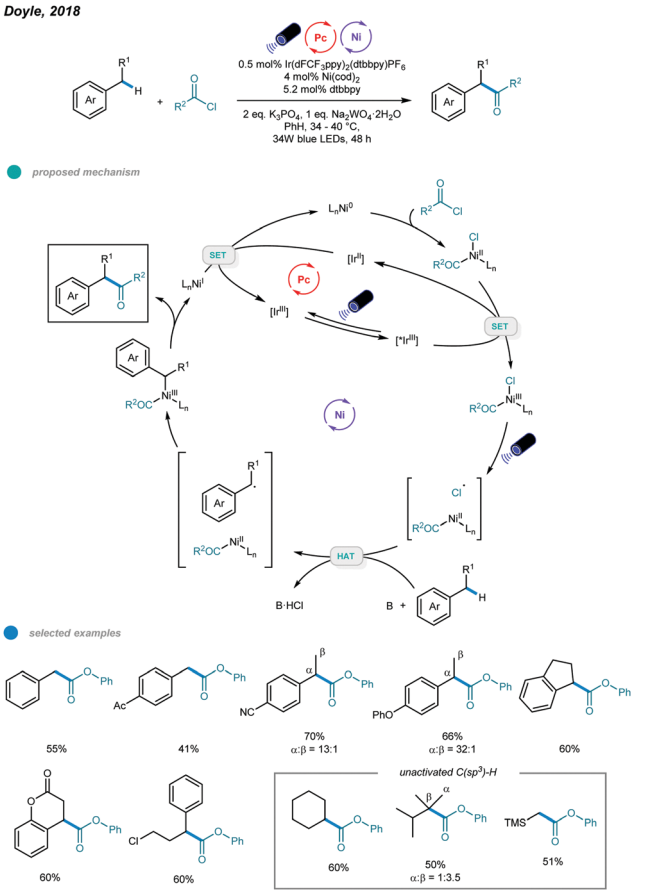

Scheme 8 Photoredox and nickel dual-catalyzed acylation of unactivated C–H bonds of alkanes and toluene derivatives.

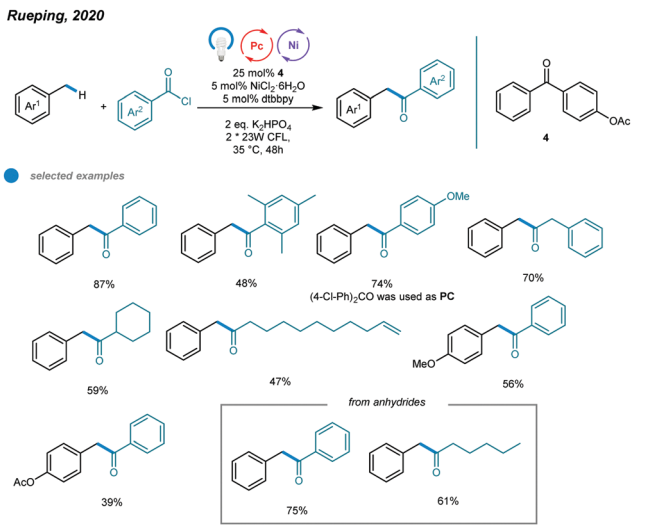

Scheme 9 Photoredox and nickel dual-catalyzed acylation of benzylic C–H bonds of toluene derivatives.

product in low yield. In addition, benzoic anhydrides, caproic anhydride and pivalic anhydride were all effective acylating reagents. This method provides a general and attractive alternative with which to access valuable ketones.

In 2020, Murakami, Ishida, and coworkers realized photoredox and nickel dual-catalyzed acylation of alkylbenzenes (Scheme 10).[45] A number of α-aryl ketones were prepared *via* a dehydrogenative coupling reaction between benzylic and aldehydic C–H bonds. Mechanistically, $Ir^{III}PF_6$ first undergoes anion exchange with $NiBr_2$ to form an $Ir^{III}Br$ complex. This $Ir^{III}Br$ complex is excited upon irradiation with blue LEDs and then undergoes SET from bromide anion to iridium(III) to afford a $Br^{\bullet}$ radical and the Ir^{II} species that reduces $NiBr_2$ to a Ni^{I}–Br species. Abstraction of benzylic and aldehydic H atoms by the resulting $Br^{\bullet}$ radical generates benzylic and acyl radical species, respectively. Addition of the two radicals to Ni^{I}–Br species forms Bn–Ni^{III}Br–acyl intermediates, which deliver the α-aryl ketone product *via* reductive elimination. Finally, the $NiBr_2$ catalyst is regenerated by reaction of the Ni^{I}–Br species and HBr with the release of H_2 gas. Electron-rich toluene derivatives, as well as methyl groups containing thiophene, furan, and indole, coupled smoothly with the aldehyde.

Notably, the challenging substrate ethylbenzene also worked with this protocol and provided the corresponding product in moderate yield. Cyclic, linear and α-branched aliphatic aldehydes were successfully applied. However, toluene derivatives bearing electron-withdrawing groups such as alkoxycarbonyl, acyl, and cyano, as well as aromatic aldehydes, gave no coupling products.

It is noted that the efficient benzylic C–H acylation of indoles has been realized by the Lee group using symmetric acid anhydrides as the acyl sources.[40]

More recently, an efficient and versatile methodology for asymmetric acylation of benzylic C–H bond was established by Huo and coworkers (Scheme 11).[46] Photoredox and nickel dual-catalyzed cross-coupling reactions of feedstock carboxylic acids and simple alkyl benzenes provide straightforward access to α-aryl ketones and α-aryl esters with high enantioselectivities. In the mechanism, the bromide anion is initially oxidized to the bromine radical *via* SET with an excited $*Ir^{III}$ photocatalyst, which forms a reducing Ir^{II} species. The bromine radical abstracts a hydrogen atom from the alkylbenzene to give a benzylic radical. Additionally, the carboxylic acid derivative undergoes oxidative addition with the active Ni^{0} catalyst to form an acyl–Ni^{II} intermediate, which traps the resulting benzylic radical to furnish an acyl–Ni^{III}–Bn intermediate. Reductive elimination from the Ni^{III} intermediate delivers the desired product and a Ni^{I} species. Finally, reduction of the Ni^{I} species by the reducing Ir^{II} species regenerates the active Ni^{0}

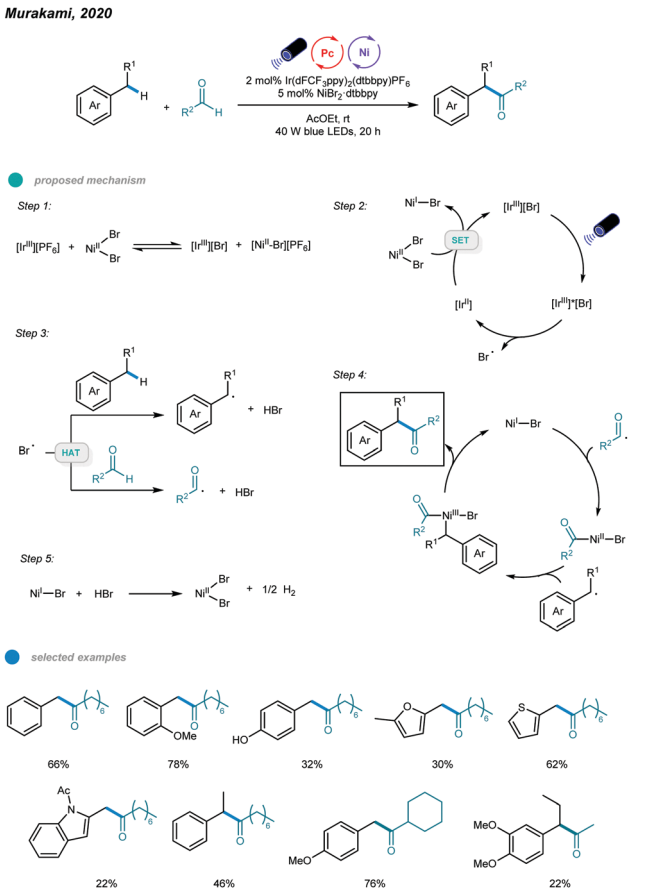

Scheme 10 Photoredox and nickel dual-catalyzed acylation of C–H bonds of alkylbenzenes with aldehydes.

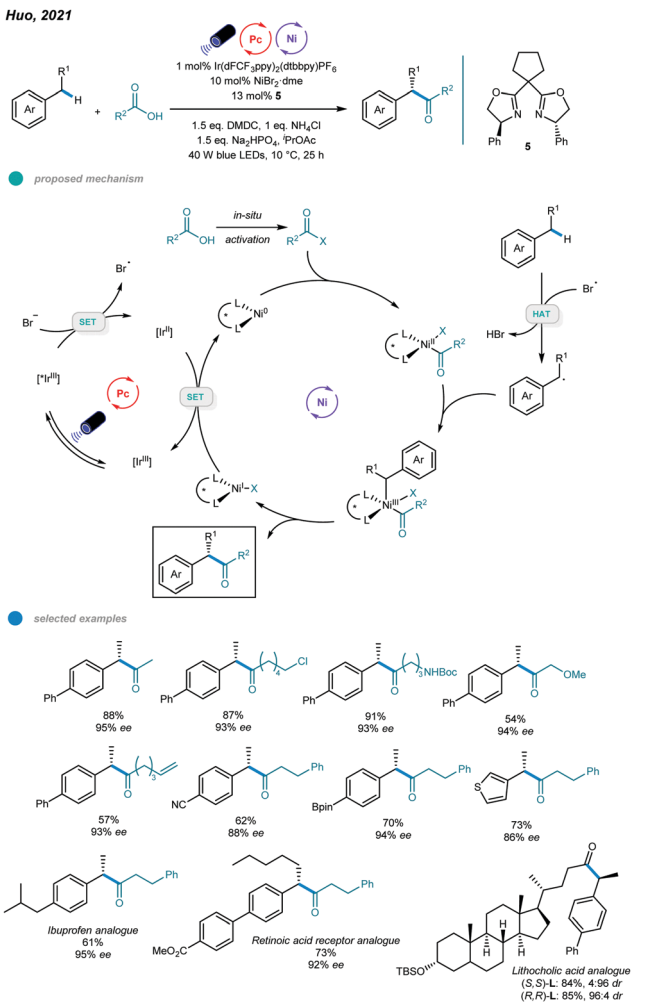

Scheme 11 Photoredox and nickel dual-catalyzed asymmetric acylations of benzylic C–H bonds with carboxylic acids.

species and completes the catalytic cycles. Reaction screening showed that the use of $NiBr_2$·glyme as a nickel source and chiral bis(oxazoline) as a ligand ensures high reactivity and enantioselectivity. The scope with regard to both carboxylic acids and alkylarenes is broad, and various functional groups, such as chloride, bromide, olefin, boronate ester, and heterocycles, were tolerated. Moreover, late-stage functionalizations of a series of pharmaceutically relevant molecules were carried out, yielding the corresponding drug analogs with moderate to good yields and high enantioselectivities. Notably, aromatic carboxylic acids participated in this reaction and gave only modest yields and enantioselectivities, and the sterically hindered coupling partners also participated inefficiently, giving low yields or no product.

4. Alkylation of benzylic and allylic C(sp^3)–H bonds

The Nozaki–Hiyama–Kishi (NHK) reaction represents one of the most powerful methods for allylation of aldehydes, but inherent drawbacks, such as stoichiometric generation of chromium waste or use of excess manganese, limit its application.[47–49] In 2018, Glorius's group reported the first photoredox- and chromium-catalyzed allylic C–H functionalization protocol for allylation of aldehydes (Scheme 12).[50] A wide array of homoallylic alcohols was synthesized with excellent diastereoselectivities *via* the reaction of aldehydes with electron-rich alkenes, including allyl (hetero)arenes, β-alkyl styrenes, and allyldiarylamines. In the mechanism, photoexcitation of Ir-based photocatalysts first gives excited state $*Ir^{III}$, which oxidizes the electron-rich alkene to a radical cation intermediate; the radical cation is deprotonated to furnish an allylic radical. The resulting allylic radical is then trapped by the Cr^{II} catalyst to form an allyl Cr^{III} intermediate, which subsequently reacts with aldehyde *via* a six-membered transition state to generate chromium alkoxide in an *anti*-selective manner. Protonolysis of chromium alkoxide delivers the homoallylic alcohol product along with a new high-valent Cr^{III} intermediate. Reduction of this Cr^{III} complex by the reducing Ir^{II} photocatalyst regenerates the active Cr^{II} catalyst and completes the catalytic cycle. Mechanistic studies, including chromium-free reactions, Stern–Volmer quenching, radical trapping, and ring-opening control experiments, suggest the formation of organochromium intermediates and support the proposed mechanism.

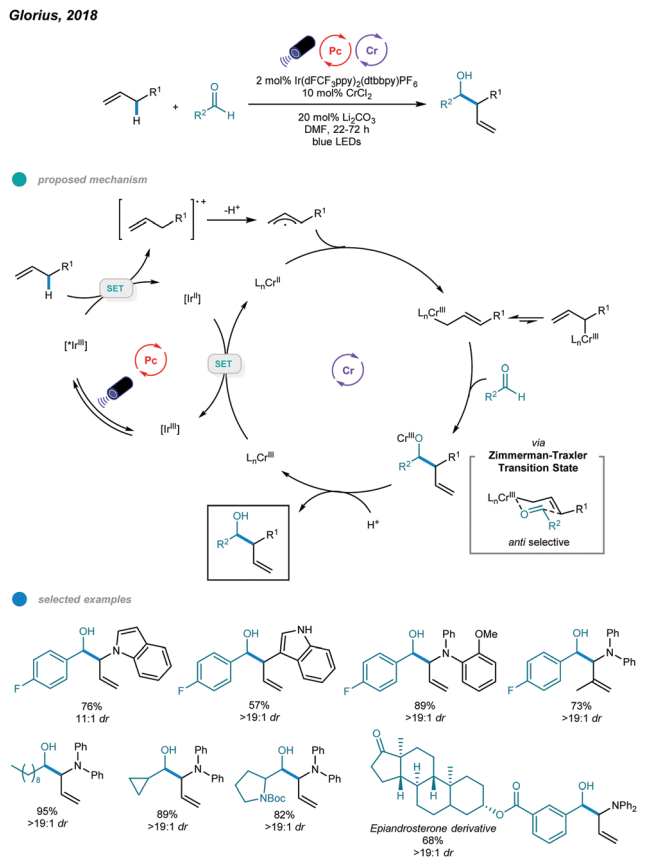

Scheme 12 Photoredox and chromium dual-catalyzed allylations of aldehydes.

A series of allyl-indoles and *N*-allyl-carbazoles, including those bearing free N–H bonds, worked well and gave the corresponding products in high yields with excellent diastereoselectivities. Other alkenes, such as electron-rich allylic benzenes, β-alkyl styrenes, and *N*-allyl-diarylamines, were also used in this allylation protocol and exhibited good efficiency. However, less electron-rich allylic benzenes afforded the C–H alkoxylated product in low yield despite the utilization of a more oxidizing photocatalyst. Linear, branched, and cyclic aliphatic aldehydes, as well as aromatic aldehydes bearing reactive halides and bulky *ortho*-substituents, all underwent this transformation and showed good yields with exclusive diastereoselectivities. Interestingly, an epiandrosterone derivative containing other types of carbonyl moieties reacted with *N*-allyl-diphenylamine with high chemoselectivity. Additionally, a scaled-up reaction was successfully performed and gave a high yield. However, although primary and secondary aliphatic aldehydes participated well in this allylation reaction, tertiary aliphatic aldehydes were ineffective substrates, probably due to steric effects.

One year later, asymmetric allylation of aldehydes was realized by Kanai and coworkers *via* photoredox and chromium dual-catalyzed allylic C(sp^3)–H functionalization of unactivated alkenes (Scheme 13).[51] A range of homoallylic alcohols was formed with excellent diastereoselectivities and enantioselectivities. The success of this protocol relies on generation of organometallic intermediates from hydrocarbon alkenes. Specifically, allyl radicals, generated from oxidation of alkenes by excited organophotoredox acridinium catalysts and subsequent deprotonation of the generated cation radicals, are trapped by the chiral chromium(II) catalyst to give a chiral allyl chromium(III) complex. The resulting chromium(III) complex undergoes nucleophilic attack with an aldehyde in a *syn*-selective fashion, forming an enantiomerically enriched chromium alkoxide that provides the desired chiral homoallylic alcohol after protonolysis. Reduction of the oxidized chromium(III) complex regenerates the active chiral chromium(II) species. Interestingly, the addition of $Mg(ClO_4)_2$ as an additive significantly improves the reactivity and enantioselectivity, which may be due to its ability to

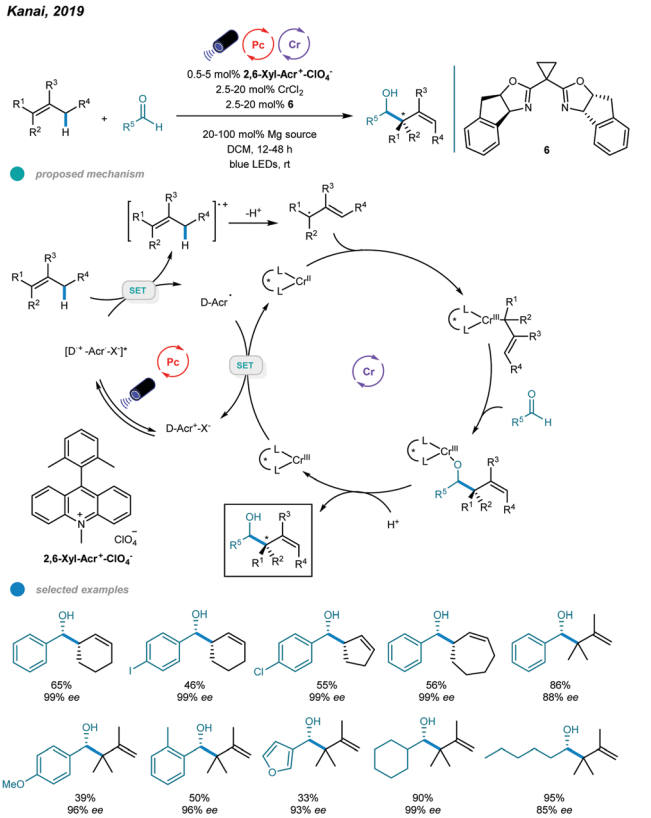

Scheme 13 Photoredox and chromium dual-catalyzed asymmetric allylations of aldehydes.

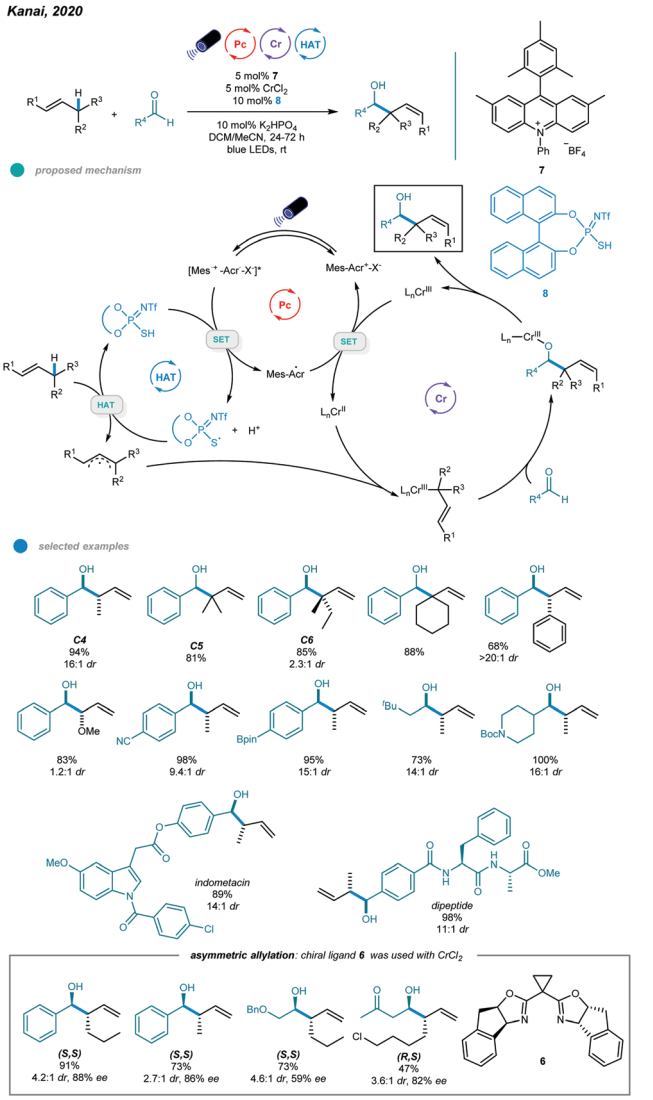

Scheme 14 Photoredox and chromium dual-catalyzed allylation of aldehydes using unactivated alkenes.

enhance the radical cation concentration. Cyclic alkenes with different ring sizes and tri- and tetrasubstituted linear alkenes all reacted with aldehydes to give the corresponding products in moderate to high yield with up to 99% ees. Aromatic aldehydes bearing electron-neutral and electron-donating functional groups, heteroaryl aldehydes, and cyclic and linear aliphatic aldehydes were all feasible substrates, delivering chiral alcohols with good to excellent yields and enantioselectivities. Notably, 10 mol% $CrCl_3{\cdot}3THF$ and 30 mol% NaO^tBu were used instead of $CrCl_3{\cdot}3THF$ for less reactive aldehydes, such as *o*-tolualdehyde and *p*-methoxybenzaldehyde, to obtain higher yields.

Although this protocol provides an efficient method for allylic functionalization of cyclic and tri- and tetrasubstituted alkenes, linear terminal alkenes and disubstituted internal alkenes such as 1-hexene and 2-butene are not functionalized. This limited scope is likely caused by their high oxidation potentials, which makes them difficult to oxidize by excited photoredox catalysts. To overcome this limitation, Kanai's group developed in 2020 a ternary hybrid catalyzed system comprising a photoredox catalyst, a hydrogen atom transfer (HAT) catalyst, and a chromium complex catalyst and realized catalytic allylation of aldehydes with even simple alkenes and structurally elaborated aldehydes (Scheme 14).[52]

Unlike the previous report in which the allyl radical was generated *via* direct oxidation of the alkene and subsequent deprotonation, the allyl radical in this process was formed *via* the HAT pathway. In particular, initial oxidation of the thiophosphoric imide (TPI) HAT catalyst by excited acridinium catalyst gives a sulfur-centered radical RS$^{\bullet}$ that abstracts a hydrogen atom from the allylic C–H bond of the alkene to afford the allyl radical. The subsequently formed allylchromium(III) species then attacks aldehydes *via* a six-membered chair transition state, furnishing the chromium alkoxides in an *anti*-selective manner. Finally, the homoallylic alcohol product is obtained after protonolysis. After screening, the authors found that the optimal reaction condition involved a combination of 5 mol% $CrCl_2$, 10 mol% TPI as the HAT catalyst, 5 mol% acridinium salt as the photocatalyst, and 10 mol% K_2HPO_4 as the base in a mixed DCM and MeCN solvent system under blue LED irradiation at room temperature for 24 h. Most linear and branched alkenes, including C4, C5, C6 feedstocks, and some internal alkenes, reacted with aldehydes in good to excellent yields with high branch- and *anti*-selectivity, which was probably caused by a six-membered chair transition state for the (*E*)-2-hexenylchromium species. Although allyl ethers also participated in this reaction and

exhibited high reactivity, the diastereoselectivity was low. The scope of aldehydes was quite broad, as illustrated by the use of aromatic and aliphatic aldehydes bearing steric and potentially sensitive functional groups and densely functionalized aldehydes, all of which participated in this process and exhibited good efficiency and diastereoselectivity. Notably, the transformation proceeded with site selectively to provide alkene C–H functionalization and leave the allylic and benzylic C–H bonds of aldehydes untouched. More importantly, the use of an indane-BOX ligand enabled catalytic asymmetric allylation of aldehydes with excellent regioselectivity, albeit with moderate to good diastereoselectivity and enantioselectivity.

In addition to photoredox and chromium dual catalysis, a combination of photoredox agents and other metals, such as copper, was also developed for alkylation of benzylic C(sp^3)–H bonds. In 2018, Wu's group reported photoredox and copper-catalyzed reactions of alkylbenzenes and enones (Scheme 15).[53] This Giese reaction between benzylic C–Hs and enones provides a convenient and efficient way to access value-added γ-aryl ketones. In this process, the benzylic radical is generated

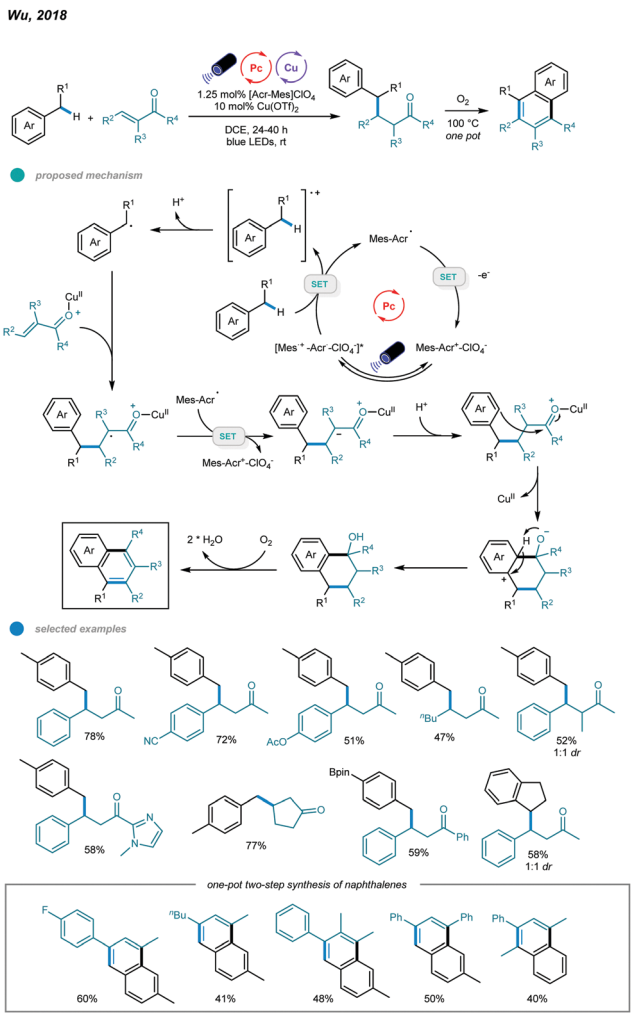

Scheme 15 Photoredox and copper dual-catalyzed Giese reactions between benzylic C(sp^3)–H and enones.

via oxidation of toluene by the excited state acridinium photocatalyst and subsequent deprotonation. Nucleophilic addition of the resulting benzylic radical to the $Cu(OTf)_2$-activated enone gives a Lewis acid alkyl radical adduct, which is then reduced by the intermediate from the acridinium catalyst to form the corresponding cation intermediate. Finally, the cation intermediate undergoes protonation to deliver the Giese adduct. The scope of enones is extremely broad, as illustrated by the fact that electron-rich and electron-deficient benzylideneacetone, β-alkylated enones, simple vinyl ketones, trisubstituted benzylideneacetones, chalcone-type enones, aryl ketones bearing heterocycles, cyclic enones bearing different ring sizes, and unsaturated esters can all be employed to furnish benzylic conjugate addition products. Methylbenzenes containing steric *ortho*-methyl substituents, boronate esters, or pyridine as well as ethylbenzene and indane underwent this transformation smoothly in the presence of the dual catalysts, affording the desired products in good yields.

More recently, asymmetric functionalization of C–H bonds in benzylic and allylic hydrocarbons, as well as in unactivated alkanes, was realized by Gong and coworkers (Scheme 16).[54] The combination of a commercially available HAT organophotocatalyst (5,7,12,14-pentacenetetrone), earth-abundant metal (Cu or Co), tunable chiral bisoxazoline ligand and blue light led to transformations occurring with good efficiency and high regio- and stereoselectivity.

A wide range of functionalized chiral products was obtained economically by reacting *N*-sulfonylimines and hydrocarbons at −20 °C. The alkyl radical is generated along with a semiquinone-type radical *via* HAT between hydrocarbons and the excited organophotocatalyst. Then, the imine-coordinated chiral metal catalyst is reduced by the semiquinone-type radical to form a metal-stabilized carbon radical, which reacts with the alkyl radical to afford a new metal intermediate. At this junction, the regio- and enantioselectivity are sterically controlled by the chiral ligand-transition metal complex. Finally, the chiral product is delivered after protonation and ligand substitution, and the imine-coordinated chiral metal catalyst is regenerated. Primary, secondary, and tertiary benzylic hydrocarbons all worked well in this reaction, affording the corresponding chiral products in 76–97% yields with high enantioselectivities. However, secondary benzylic hydrocarbons showed no diastereoselectivity. Toluene-type substrates bearing halogen, ester, boron ester, ketone, and amide groups, as well as diversely substituted alkylbenzenes, all produced the desired products and exhibited excellent reactivities and enantioselectivities.

Moreover, a number of tri- and tetrasubstituted alkenes also underwent this asymmetric C–H functionalization and showed good yields with moderate to high ee values, albeit with a higher catalyst loading and reaction temperature and a long reaction time (3–5 days). Notably, the application of other nonprecious transition metals, including zinc, nickel, and cobalt, led to inverted enantioselectivities compared to those of a copper complex used with the same chiral ligand and identical reaction conditions, providing the possibility for development of stereodivergent syntheses by employing different metals. Moreover, late-stage modification of medicinal agents,

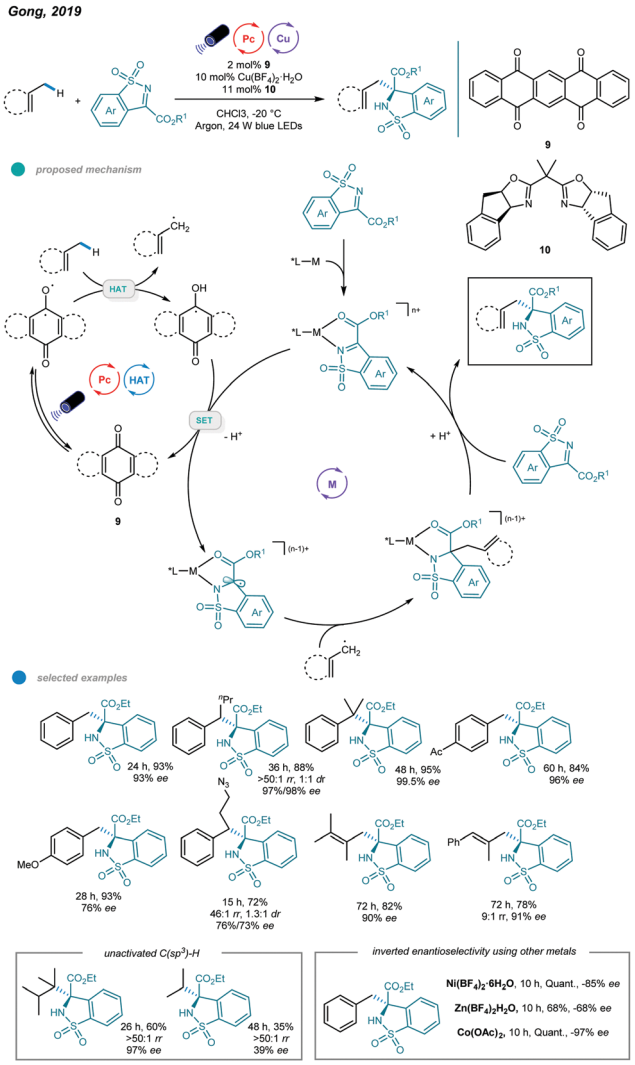

Scheme 16 Photoredox and copper dual-catalyzed asymmetric C–H functionalizations of hydrocarbons with *N*-sulfonylimines.

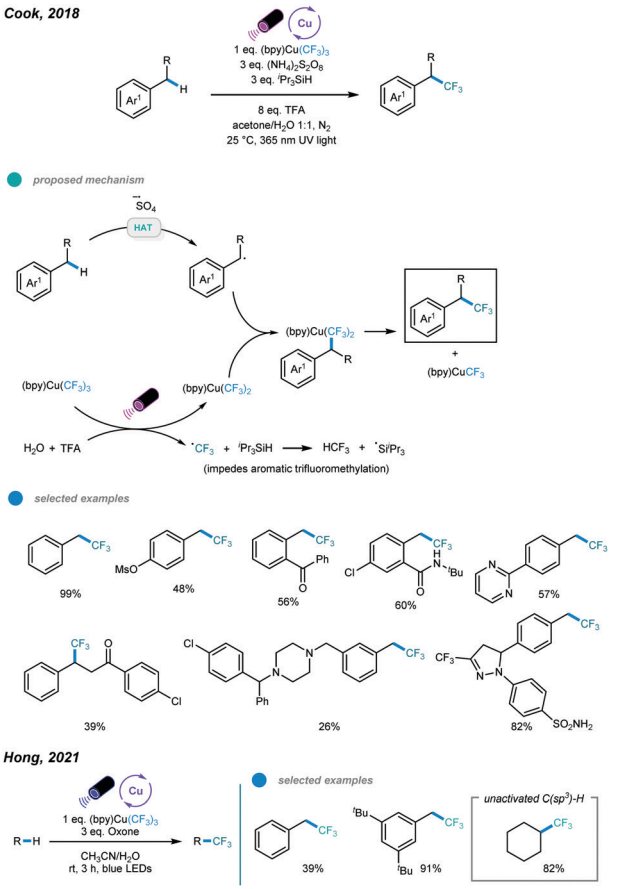

Scheme 17 C(sp^3)–H trifluoromethylation by trifluoromethyl copper complexes.

including Celebrex, a Lopid derivative, and Skelaxin, afforded chiral products with good activity and enantioselectivity.

In 2018, an UV light induced benzylic C–H trifluoromethylation has been developed by Cook and coworkers using Grushin's reagent in an acetone/water solvent system (Scheme 17).[55] UV light irradiation results in the generation of an active (bpy)Cu(CF_3)$_2$ *via* hemolysis of the Grushin's reagent and sulfate radical anion from ammonium persulfate. The HAT event between the sulfate radical anion and benzylic C–H bond gives a benzylic radical. The resulting benzylic radical is intercepted by the active (bpy)Cu(CF_3)$_2$ to form a Bn–(bpy)Cu(CF_3)$_2$ complex, which undergoes subsequent reductive elimination to furnish the benzylic C–H trifluoromethylation product. Both primary and secondary benzylic C–H bonds could undergo this trifluoromethylation reaction smoothly. Typically, primary benzylic C–H bonds have a faster reaction rate and give the corresponding products in higher yields. Notably, late-stage C–H trifluoromethylation of bioactive molecules have also been successfully performed. However, tertiary benzylic C–H bonds showed no reactivity. Later on, using Grushin's reagent, the Hong group realized the direct C(sp^3)–H trifluoromethylation of unactivated alkanes with the aid of an oxone as additive under the irradiation of blue LED, in which o examples of benzylic C(sp^3)–H trifluoromethylation have been included (Scheme 17).[56]

Very recently, methylation of benzylic and α-amino C(sp^3)–H bonds *via* photo/nickel dual catalysis has been reported by Stahl and coworkers (Scheme 18).[57] Mechanistically, visible light-initiated triplet energy transfer between photocatalyst and di-*tert*-butyl peroxide (DTBP) leads to the generation of alkoxyl radicals, which could undergo either β-methyl scission to generate a methyl radical, or hydrogen-atom transfer (HAT) with the C(sp^3)–H bond to generate a benzylic or α-amino radical. At last, the methylation product is formed *via* the cross-coupling of the resulting two types of radicals with the aid of nickel catalyst. A series of activated C–H substrates as well as α-amino substrates including medicinally relevant building blocks and drug molecules all could be methylated smoothly.

5. Carboxylation of benzylic and allylic C(sp^3)–H bonds

The fixation of CO_2 into organic skeletons *via* C–C bond formation has always been an appealing approach. In particular,

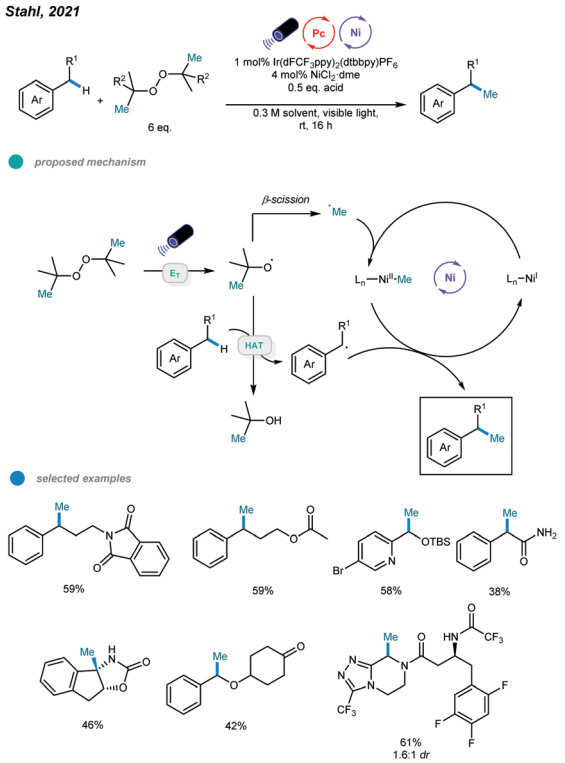

Scheme 18 Photo and nickel dual-catalyzed benzylic and α-amino C(sp^3)–H bonds methylation reactions.

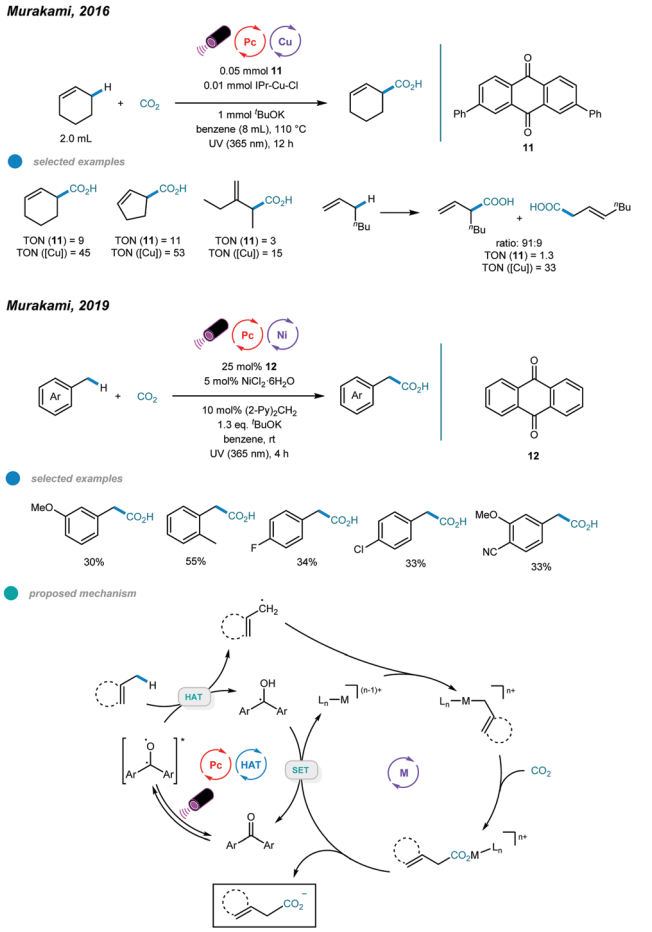

Scheme 19 Photoredox and copper/nickel dual-catalyzed benzylic and allylic C(sp^3)–H carboxylation.

directly fixing CO_2 into readily available hydrocarbons remains more intriguing. In 2016, Murakami and coworkers used a combination of ketone photosensitizer and copper catalyst and realized a photoinduced carboxylation reaction between allylic C–H bonds of simple alkenes and CO_2 (Scheme 19).[58] The reaction was conducted at 110 °C under UV irradiation and with K^{t}OBu as the base. The catalytic cycle starts with generation of an excited ketone *via* UV irradiation of the ketone photosensitizer. Abstraction of an allylic hydrogen from an alkene gives a geminate radical pair that is prone to undergo radical–radical coupling to form the tertiary homoallylic alcohol. The homoallylic alcohol is then deprotonated by copper *tert*-butoxide to form a copper alkoxide intermediate, and then β-carbon elimination furnishes an allyl copper species. Nucleophilic addition of the resulting allyl copper species to CO_2 affords a copper carboxylate that undergoes ligand exchange with K^{t}OBu to deliver the carboxylate salt and regenerate active copper *tert*-butoxide. Several cyclic and linear alkenes were used with moderate to good efficiency. It is worth noting that branched carboxylic acid isomers were favored products.

However, when toluene derivatives containing benzylic C–H bonds were employed, no carboxylation product was observed. In 2019, the Murakami group extended the scope to benzylic C–H bonds by changing the metal from copper to nickel (Scheme 19).[59] The combination of xanthone photosensitizer, $NiCl_2{\cdot}6H_2O$ metal catalyst, di(2-pyridyl)methane ligand, K^{t}OBu base, benzene solvent, and irradiation with UV LED lamps (λ_{max} = 365 nm) enabled carboxylation of toluene derivatives under one atmosphere of CO_2 at room temperature. Herein, the excited xanthone abstracts a hydrogen atom from the benzylic C–H bond to give a benzylic radical that adds to the active Ni^0 catalyst to afford a benzyl-Ni^I species. The resulting Ni^I species traps one molecule of carbon dioxide to give a Ni^I carboxylate, and then SET with a ketyl radical anion furnishes the carboxylate anion and regeneration of the active Ni^0 species and the ground state ketone. A ring opening experiment with cyclopropylmethylanisole was carried out, and the acyclic carboxylic acid was the major product, indicating the involvement of benzylic radicals and thus supporting the proposed mechanism. A range of methylbenzene derivatives was tested, and monocarboxylated products were generated exclusively for all substrates. *ortho*-Methyl groups and halides, including fluoride and chloride, were all tolerated. However, the carboxylation reaction of ethylbenzene showed low efficiency, giving carboxylic acid in only 15% yield; this requires further improvement.

6. Alkynylation of allylic C(sp^3)–H bonds

1,4-Enynes constitute a class of useful synthons that is important in organic synthesis. In 2020, Mejía and coworkers

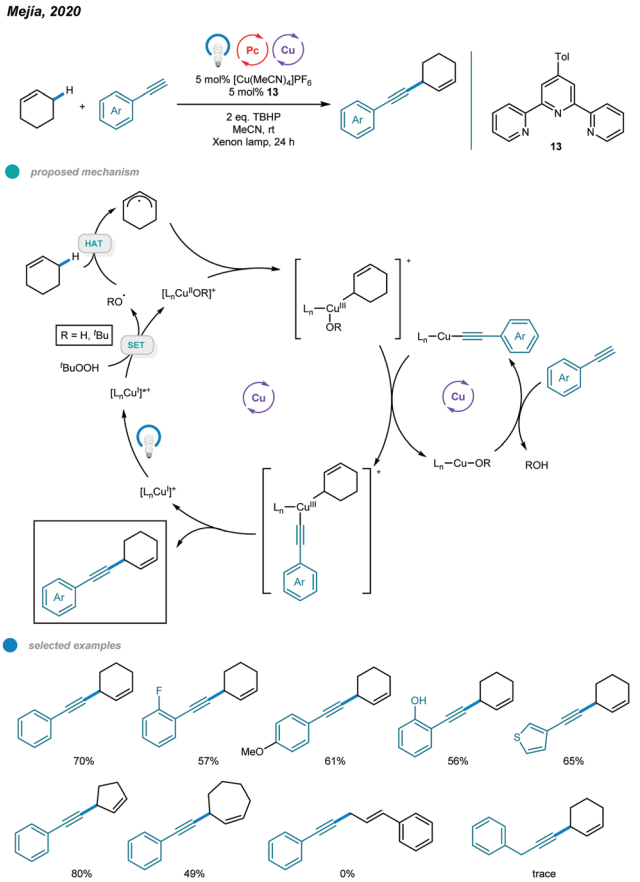

Scheme 20 Photoredox and copper dual-catalyzed allylic C–H alkynylations.

reported photoinduced copper-catalyzed cross-dehydrogenative coupling (CDC) for allylic C–H alkynylation (Scheme 20).[60] A series of valuable 1,4-enynes was prepared *via* coupling of cyclic alkenes and aryl alkynes in a one-step process involving 5 mol% of a copper(I) terpyridyl complex as the photocatalyst, two equivalents of DTBP (di-*tert*-butylperoxide) as the oxidant and irradiation with white light (xenon lamp, λ = 300–700 nm) at room temperature. In the mechanism, $[LCu^{I}]^{+}$ is first converted to excited $[LCu^{I}]^{+*}$ upon irradiation with white light. The excited copper species then undergoes SET with DTBP, producing an oxidized $[LCu^{II}OR']^{+}$ complex and R′O• radical. The R′O• radical abstracts a hydrogen atom from the C–H bond of the cyclic alkene, generating an allylic radical that is trapped by the oxidized $[LCu^{II}OR']^{+}$ complex to afford a Cu^{III} intermediate. The Cu^{III} intermediate undergoes ligand exchange with the organocuprate LCu-alkyne to produce a new Cu^{III} complex that undergoes reductive elimination and delivers the CDC product with regeneration of the active $[LCu^{I}]^{+}$ catalyst. Alkynes bearing *ortho*-, active- and heterocyclic substituents all worked well in this system. Cyclic alkenes with different ring sizes were alkynylated smoothly. However, the C–H bonds of internal alkenes and aliphatic alkynes were not feasible substrates for this allylic C–H alkynylation protocol.

7. Sulfonylation and azidation of benzylic C(sp^3)–H bonds

Although a series of two-component transformations giving C–C bond formation based on C(sp^3)–H activation have been established *via* metallaphotocatalysis, protocols for C-heteroatom bond formation and three-component reactions remain undeveloped. Very recently, Gong and coworkers reported a photoredox and nickel dual-catalyzed three-component reaction involving a C(sp^3)–H precursor, a SO_2 surrogate and a common α,β-unsaturated carbonyl compound (Scheme 21).[61] The application of a well-tailored chiral bisoxazoline ligand enabled the asymmetric three-component sulfonylation reaction, and a series of α-C chiral sulfones was prepared. (DABCO·$(SO_2)_2$) was found to be an efficient SO_2 surrogate in this cascade protocol.

Mechanistically, the chiral nickel catalyst L*-Ni^{II} first coordinates with the α,β-unsaturated *N*-acylpyrazole to form a new Ni^{II} complex. Additionally, the transient carbon radical

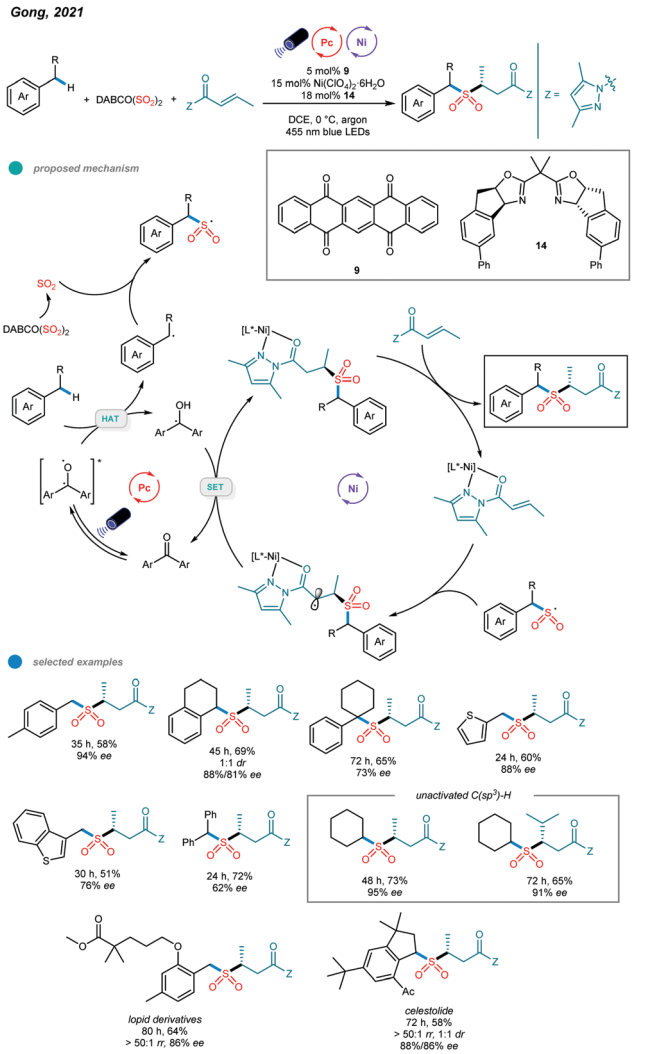

Scheme 21 Photoredox and nickel dual-catalyzed three-component sulfonylations of C–H bonds of alkylbenzenes.

generated from HAT with the excited organophotocatalyst is trapped by the sulfur dioxide released *in situ* to give the stable sulfonyl radical. The addition of the sulfonyl radical to the metal-coordinated Michael acceptor produces a metal-coordinated radical species, which undergoes a SET reduction with the semiquinone-type radical intermediate, and subsequent protonation affords the chiral sulfonylation product. In addition to alkanes, alkylbenzenes bearing primary, secondary, tertiary and benzylic C(sp^3)–H bonds as well as methyl-substituted heterocycles all worked well in this asymmetric cascade reaction, providing the desired products in good yields with moderate to high enantioselectivities. Significantly, late-stage modifications of a Lopid derivative and Celestolide were accomplished with good yields and ee values.

Notably, by merging metal catalysis, electrocatalysis, and photocatalysis, Lei and coworkers realized manganese-catalyzed oxidative azidation of C(sp^3)–H bonds (Scheme 22).[62] This electrophotocatalytic protocol supports installation of synthetically useful azide groups into alkylbenzenes and simple alkanes while using nucleophilic NaN_3 as an azide source under mild conditions. In this protocol, the benzylic radical was produced *via* HAT with either an excited organophotocatalyst or azide radical generated from anodic oxidation of NaN_3. For the Mn catalytic cycle, initial ligand exchange of N_3^- with Mn^{II}(L) gives an N3-MnII(L) intermediate, which undergoes anodic oxidation to form an N_3-Mn^{III}(L) intermediate. Subsequent azide transfer from the N_3-Mn^{III}(L) intermediate to a benzylic radical delivers the azidation product. An array of tertiary and secondary benzyl C(sp^3)–H was applied, and moderate to excellent yields were obtained. Heterocycles bearing secondary benzyl C(sp^3)–H bonds, indane, and long-chain alkyl-substituted benzenes were all effective candidates. Notably, a scale-up reaction run on a 10 mmol scale proceeded smoothly and with good yield. This electrophotocatalytic protocol opens a new avenue allowing chemists to address some challenging organic syntheses that are difficult to realize with traditional methodologies.

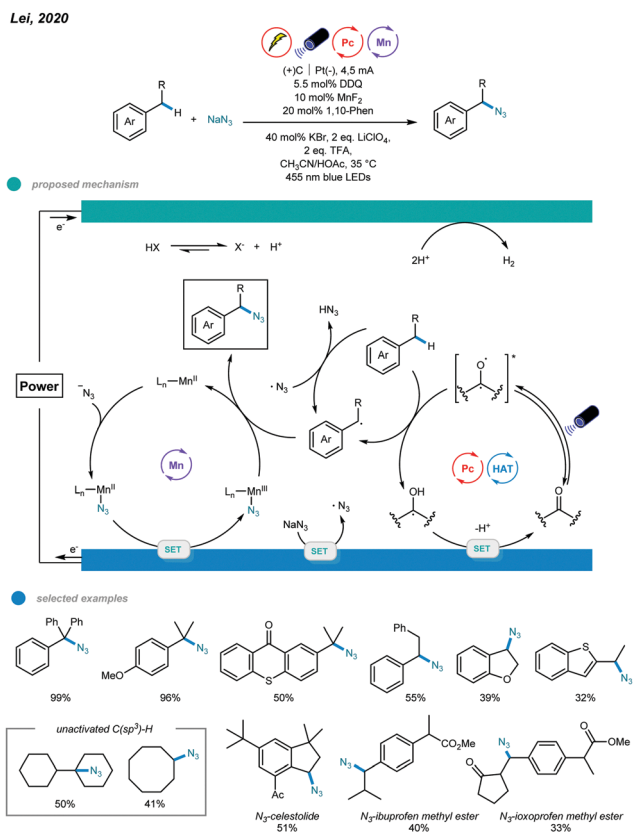

Scheme 22 Manganese catalyzed oxidative azidation of C(sp^3)–H bonds *via* electrophotocatalysis.

8. Conclusion and outlook

In this feature article, we have highlighted the recent progress seen with metallaphoto-catalyzed functionalization of benzylic and allylic C(sp^3)–H bonds. The newly developed approaches have been classified according to the type of transformation, including arylation, acylation, alkylation, carboxylation, alkynylation, sulfonylation and azidation. The illustrated methodologies enable the application of abundant hydrocarbons such as ethylbenzenes and alkenes as coupling partners in transition-metal catalyzed reactions. The transformations of more native functionalities to high-value compounds and the advantages of step and atom economy made these protocols appealing. The mild benzylic and allylic radical generating pathways involving HAT or SET allow the reactions to occur under very mild conditions, proceed with good chemo- and regioselectivity and illustrate good functional group compatibility. In some cases, an excess of C–H substrate is required for the transformations, possibly to boost the rate of bimolecular HAT and compete with radical annihilations. Future studies should focus on a few key challenges. First, the mechanism should be investigated in more detail since different research groups have described slightly different mechanisms for similar transformations. Second, compared to C–C bond formation, C-heteroatom bond formation *via* benzylic and allylic C(sp^3)–H activation remains undeveloped and deserves more attention. Additionally, from the standpoint of practicability, more heterogeneous catalytic modes employing reusable photocatalysts should be developed. Moreover, considering the exclusive advantages of electrocatalysis, a combination of electro- or photoelectrocatalysis with C–H bond activation would be attractive. In addition, more effort should be dedicated to developing other efficient chiral ligands for asymmetric C–H bond functionalization and using benzylic and allylic radicals in more multicomponent reactions.

Conflicts of interest

There are no conflicts to declare.

Acknowledgements

This work was financially supported by the King Abdullah University of Science and Technology (KAUST), Saudi Arabia, Office of Sponsored Research (URF/1/4384).

Notes and references

1 T. Rogge, N. Kaplaneris, N. Chatani, J. Kim, S. Chang, B. Punji, L. L. Schafer, D. G. Musaev, J. Wencel-Delord, C. A. Roberts, R. Sarpong, Z. E. Wilson, M. A. Brimble, M. J. Johansson and L. Ackermann, *Nat. Rev. Methods Primers*, 2021, **1**, 43.
2 P. Gandeepan, T. Müller, D. Zell, G. Cera, S. Warratz and L. Ackermann, *Chem. Rev.*, 2018, **119**, 2192–2452.
3 L. Ackermann, *Chem. Rev.*, 2011, **111**, 1315–1345.
4 C. Sambiagio, D. Schönbauer, R. Blieck, T. Dao-Huy, G. Pototschnig, P. Schaaf, T. Wiesinger, M. F. Zia, J. Wencel-Delord and T. Besset, *Chem. Soc. Rev.*, 2018, **47**, 6603–6743.
5 T. Gensch, M. Hopkinson, F. Glorius and J. Wencel-Delord, *Chem. Soc. Rev.*, 2016, **45**, 2900–2936.
6 G. Rouquet and N. Chatani, *Angew. Chem., Int. Ed.*, 2013, **52**, 11726–11743.
7 J. Yamaguchi, A. D. Yamaguchi and K. Itami, *Angew. Chem., Int. Ed.*, 2012, **51**, 8960–9009.
8 R. Giri, B.-F. Shi, K. M. Engle, N. Maugel and J.-Q. Yu, *Chem. Soc. Rev.*, 2009, **38**, 3242–3272.
9 X. Chen, K. M. Engle, D. H. Wang and J. Q. Yu, *Angew. Chem., Int. Ed.*, 2009, **48**, 5094–5115.
10 J. He, M. Wasa, K. S. Chan, Q. Shao and J.-Q. Yu, *Chem. Rev.*, 2017, **117**, 8754–8786.
11 R. R. Karimov and J. F. Hartwig, *Angew. Chem., Int. Ed.*, 2018, **57**, 4234–4241.
12 K. Liao, S. Negretti, D. G. Musaev, J. Bacsa and H. M. Davies, *Nature*, 2016, **533**, 230–234.
13 C. Le, Y. Liang, R. W. Evans, X. Li and D. W. MacMillan, *Nature*, 2017, **547**, 79–83.
14 F.-L. Zhang, K. Hong, T.-J. Li, H. Park and J.-Q. Yu, *Science*, 2016, **351**, 252–256.
15 J. He, S. Li, Y. Deng, H. Fu, B. N. Laforteza, J. E. Spangler, A. Homs and J.-Q. Yu, *Science*, 2014, **343**, 1216–1220.
16 H. Yi, G. Zhang, H. Wang, Z. Huang, J. Wang, A. K. Singh and A. Lei, *Chem. Rev.*, 2017, **117**, 9016–9085.
17 A. Hu, J.-J. Guo, H. Pan and Z. Zuo, *Science*, 2018, **361**, 668–672.
18 J. M. Narayanam and C. R. Stephenson, *Chem. Soc. Rev.*, 2011, **40**, 102–113.
19 D. Ravelli, S. Protti and M. Fagnoni, *Chem. Rev.*, 2016, **116**, 9850–9913.
20 J. Xuan and W. J. Xiao, *Angew. Chem., Int. Ed.*, 2012, **51**, 6828–6838.
21 C. Zhu, H. Yue, L. Chu and M. Rueping, *Chem. Sci.*, 2020, **11**, 4051–4064.
22 C. Zhu, H. Yue, J. Jia and M. Rueping, *Angew. Chem., Int. Ed.*, 2021, **60**, 17810–17831.
23 C. K. Prier, D. A. Rankic and D. W. MacMillan, *Chem. Rev.*, 2013, **113**, 5322–5363.
24 J. Twilton, P. Zhang, M. H. Shaw, R. W. Evans and D. W. MacMillan, *Nat. Rev. Chem.*, 2017, **1**, 1–19.
25 J. C. Tellis, C. B. Kelly, D. N. Primer, M. Jouffroy, N. R. Patel and G. A. Molander, *Acc. Chem. Res.*, 2016, **49**, 1429–1439.
26 N. Holmberg-Douglas and D. A. Nicewicz, *Chem. Rev.*, 2021, DOI: 10.1021/acs.chemrev.1021c00311.
27 L. Capaldo, D. Ravelli and M. Fagnoni, *Chem. Rev.*, 2021, DOI: 10.1021/acs.chemrev.1021c00263.
28 H. Cao, X. Tang, H. Tang, Y. Yuan and J. Wu, *Chem. Catal.*, 2021, **1**, 523–598.
29 M.-M. Zhang, Y.-N. Wang, L.-Q. Lu and W.-J. Xiao, *Trends Chem.*, 2020, **2**, 764–775.
30 L. Mantry, R. Maayuri, V. Kumar and P. Gandeepan, *Beilstein J. Org. Chem.*, 2021, **17**, 2209–2259.
31 L. Guillemard and J. Wencel-Delord, *Beilstein J. Org. Chem.*, 2020, **16**, 1754–1804.
32 M. H. Shaw, V. W. Shurtleff, J. A. Terrett, J. D. Cuthbertson and D. W. MacMillan, *Science*, 2016, **352**, 1304–1308.
33 D. R. Heitz, J. C. Tellis and G. A. Molander, *J. Am. Chem. Soc.*, 2016, **138**, 12715–12718.
34 B. J. Shields and A. G. Doyle, *J. Am. Chem. Soc.*, 2016, **138**, 12719–12722.
35 N. Ishida, Y. Masuda, N. Ishikawa and M. Murakami, *Asian J. Org. Chem.*, 2017, **6**, 669–672.
36 L. Huang and M. Rueping, *Angew. Chem., Int. Ed.*, 2018, **57**, 10333–10337.
37 A. Dewanji, P. E. Krach and M. Rueping, *Angew. Chem., Int. Ed.*, 2019, **58**, 3566–3570.
38 I. B. Perry, T. F. Brewer, P. J. Sarver, D. M. Schultz, D. A. DiRocco and D. W. MacMillan, *Nature*, 2018, **560**, 70–75.
39 Y. Shen, Y. Gu and R. Martin, *J. Am. Chem. Soc.*, 2018, **140**, 12200–12209.
40 W. Kim, J. Koo and H. G. Lee, *Chem. Sci.*, 2021, **12**, 4119–4125.
41 X. Cheng, H. Lu and Z. Lu, *Nat. Commun.*, 2019, **10**, 3549.
42 X. Cheng, T. Li, Y. Liu and Z. Lu, *ACS Catal.*, 2021, **11**, 11059–11065.
43 L. K. Ackerman, J. I. Martinez Alvarado and A. G. Doyle, *J. Am. Chem. Soc.*, 2018, **140**, 14059–14063.
44 P. E. Krach, A. Dewanji, T. Yuan and M. Rueping, *Chem. Commun.*, 2020, **56**, 6082–6085.
45 T. Kawasaki, N. Ishida and M. Murakami, *J. Am. Chem. Soc.*, 2020, **142**, 3366–3370.
46 L. Huan, X. Shu, W. Zu, D. Zhong and H. Huo, *Nat. Commun.*, 2021, **12**, 3536.
47 Y. Okude, S. Hirano, T. Hiyama and H. Nozaki, *J. Am. Chem. Soc.*, 1977, **99**, 3179–3181.
48 K. Namba, J. Wang, S. Cui and Y. Kishi, *Org. Lett.*, 2005, **7**, 5421–5424.
49 A. Fürstner and N. Shi, *J. Am. Chem. Soc.*, 1996, **118**, 12349–12357.
50 J. L. Schwarz, F. Schäfers, A. Tlahuext-Aca, L. Lückemeier and F. Glorius, *J. Am. Chem. Soc.*, 2018, **140**, 12705–12709.
51 H. Mitsunuma, S. Tanabe, H. Fuse, K. Ohkubo and M. Kanai, *Chem. Sci.*, 2019, **10**, 3459–3465.
52 S. Tanabe, H. Mitsunuma and M. Kanai, *J. Am. Chem. Soc.*, 2020, **142**, 12374–12381.
53 H. Liu, L. Ma, R. Zhou, X. Chen, W. Fang and J. Wu, *ACS Catal.*, 2018, **8**, 6224–6229.
54 Y. Li, M. Lei and L. Gong, *Nat. Catal.*, 2019, **2**, 1016–1026.
55 S. Guo, D. I. AbuSalim and S. P. Cook, *J. Am. Chem. Soc.*, 2018, **140**, 12378–12382.
56 G. Choi, G. S. Lee, B. Park, D. Kim and S. H. Hong, *Angew. Chem.*, 2021, **133**, 5527–5534.
57 A. Vasilopoulos, S. W. Krska and S. S. Stahl, *Science*, 2021, **372**, 398–403.
58 N. Ishida, Y. Masuda, S. Uemoto and M. Murakami, *Chem. – Eur. J.*, 2016, **22**, 6524–6527.
59 N. Ishida, Y. Masuda, Y. Imamura, K. Yamazaki and M. Murakami, *J. Am. Chem. Soc.*, 2019, **141**, 19611–19615.
60 A. A. Almasalma and E. Mejía, *Synthesis*, 2020, 529–536.
61 S. Cao, W. Hong, Z. Ye and L. Gong, *Nat. Commun.*, 2021, **12**, 2377.
62 L. Niu, C. Jiang, Y. Liang, D. Liu, F. Bu, R. Shi, H. Chen, A. D. Chowdhury and A. Lei, *J. Am. Chem. Soc.*, 2020, **142**, 17693–17702.

